Check for updates

View Article Online
View Journal

Chemical Science

Accepted Manuscript

This article can be cited before page numbers have been issued, to do this please use: J. Arvidson, S. Shaikh, M. Tanaka, T. Pawale, A. Dawson, X. Li, V. Nesterov, Y. Kobori, S. Das and H. Wang, *Chem. Sci.*, 2026, DOI: 10.1039/D5SC08246C.

This is an Accepted Manuscript, which has been through the Royal Society of Chemistry peer review process and has been accepted for publication.

Accepted Manuscripts are published online shortly after acceptance, before technical editing, formatting and proof reading. Using this free service, authors can make their results available to the community, in citable form, before we publish the edited article. We will replace this Accepted Manuscript with the edited and formatted Advance Article as soon as it is available.

You can find more information about Accepted Manuscripts in the Information for Authors.

Please note that technical editing may introduce minor changes to the text and/or graphics, which may alter content. The journal's standard Terms & Conditions and the Ethical guidelines still apply. In no event shall the Royal Society of Chemistry be held responsible for any errors or omissions in this Accepted Manuscript or any consequences arising from the use of any information it contains.

ROYAL SOCIETY OF CHEMISTRY

rsc.li/chemical-science

Please do not adjust margins

View Article Online
DOI: 10.1039/D5SC08246C

ARTICLE

Linearly Acenaphthylene-Fused Pentacene Exhibiting Efficient Singlet Fission

Received 00th January 20xx,
Accepted 00th January 20xx

DOI: 10.1039/x0xx00000x

Jacob Arvidson,[‡a] Saad Shaikh,[‡a] Masahiro Tanaka,[‡c] Tejal Pawale,[b] Andrew Dawson,[a] Xiao Li,[b] Vladimir N. Nesterov,[a] Yasuhiro Kobori,*[c,d] Somnath Das*[a] and Hong Wang*[a]

Acenes are poised to be highly sought after for singlet fission, which is among the most promising strategies for scaling solar power conversion efficiency beyond Shockley–Queisser limit. One critical problem associated with acenes is their low stability. Incorporation of a 5-membered ring into acenes is reported to stabilize acenes. However, cyclopentannulation on acenes at the peri-positions also transforms the electronic structure of acenes and endows them with nontypical photophysical properties, thus preventing them from undergoing singlet fission. Here, we report a new strategy to stabilize and simultaneously retain the photophysical properties of the acenes through linearly fusing acenaphthylene containing a 5-membered ring. The acenaphthylene-fused pentacenes exhibited UV-Vis absorption and fluorescence spectra with distinctively red-shifted absorption and emission bands, notably along with a substantially longer fluorescence lifetime, while still retaining the characteristic spectral features of pentacene. Despite possessing narrower HOMO-LUMO energy gaps and elevated HOMO energy levels, the elongated acenes exhibited stability comparable to that of their pentacene analogues. X-ray crystallography revealed a slip-stack columnar array in these molecules, a packing motif that differs significantly from the herringbone packing typically seen in pentacene. Strong vibronic coupling—the interrelation of electronic and vibrational motions—and favorable excited-state energetics drive an efficient, ultrafast singlet fission in thin films, resulting in a high triplet quantum yield of ~158%. TREPR spectroscopy confirmed the singlet fission mechanism—specifically the formation of triplet pairs—by resolving the sequence of spin-state changes and revealing the elusive quintet (^{5}TT) state.

Introduction

Acenes are a unique class of polycyclic aromatic hydrocarbons (PAHs) composed of linearly fused benzene rings. Organic electronic materials based on acenes show promise to make revolutionary transformations in a range of applications[1–10] such as photovoltaics, organic field-effect transistors (OFETs), and light-emitting devices (OLEDs) due to their exceptional charge mobility. In photovoltaics, acenes are considered benchmark compounds for singlet fission,[11–16] a spin-conserving phenomenon to distribute one high-energy singlet exciton into a pair of twice (or even more) times lower-energy triplets, thereby effectively circumventing the Shockley-Queisser limit (~33.7%) in solar cells.[17–22] One unique and interesting feature of acenes is that their charge mobility increases exponentially with the increase in their length. As such, it has

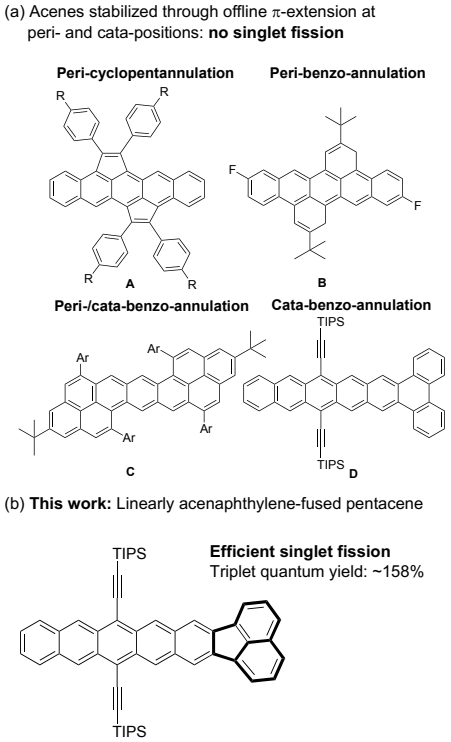

Figure 1. Selected examples of acenes stabilized through offline π-extension.

[a] Department of Chemistry, University of North Texas, Denton, TX 76203, USA
[b] Materials Science and Engineering Department, University of North Texas, 3940 North Elm Str, Denton, Texas 76209, United States.
[c] Department of Chemistry, Graduate School of Science, Kobe University, 1-1 Rokkodaicho Nada-ku Kobe, 657-8501, Japan.
[d] Laser Molecular Photoscience Laboratory, Molecular Photoscience Research Center, Kobe University, 1-1 Rokkodaicho Nada-ku Kobe, 657-8501, Japan.
[‡] J. Arvidson, S. Shaikh and M. Tanaka contribute equally to this work
Supplementary Information available: [details of any supplementary information available should be included here]. See DOI: 10.1039/x0xx00000x

Open Access Article. Published on 02 June 2026. Downloaded on 6/4/2026 9:29:30 PM.
This article is licensed under a Creative Commons Attribution 3.0 Unported Licence.

Chemical Science Accepted Manuscript

Please do not adjust margins

View Article Online
DOI: 10.1039/D5SC08246C

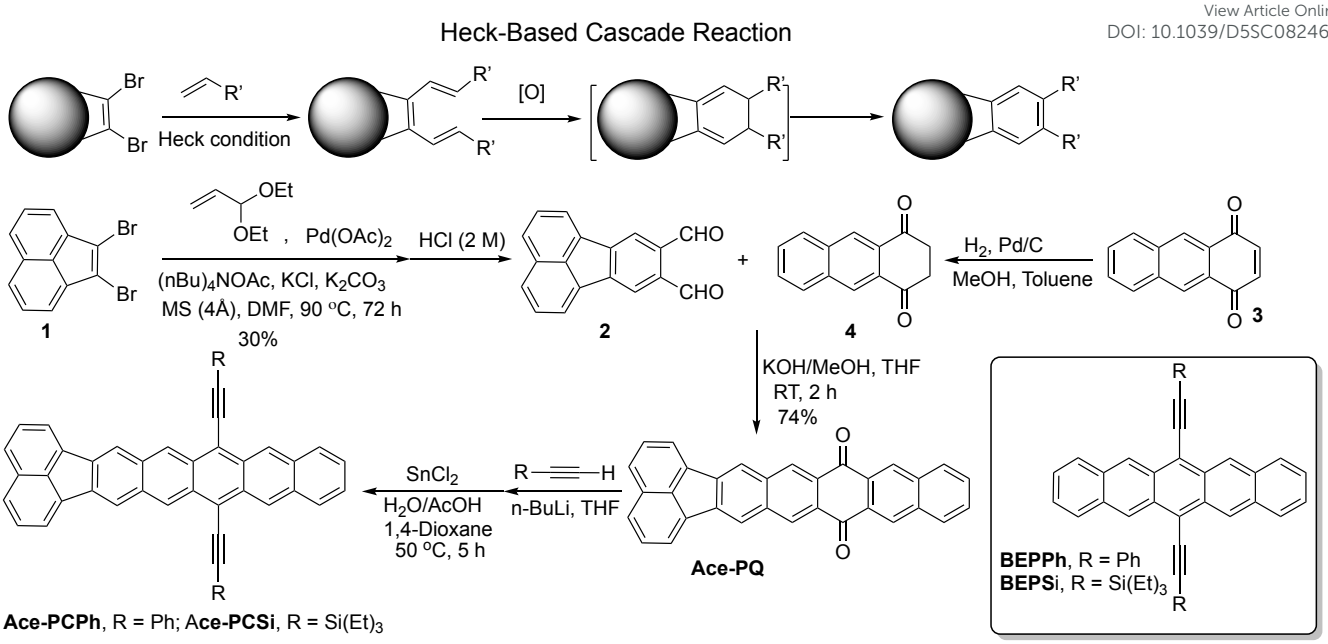

Scheme 1. Synthesis of the acenaphthylene-fused pentacenes Ace-PCPh and Ace-PCSi.

remained a hot research topic to obtain higher acenes.[2,5,15,23–38] However, a critical problem associated with higher acenes is their low stability. As the length of acenes increases, the stability drops quickly due to much more facile oxidative decomposition arising from the quickly shrinking HOMO–LUMO gap. Significant research effort has focused on this area, and strategies such as increasing steric bulkiness and substitution with strongly electron-withdrawing groups have been developed to stabilize acenes.[23,24,26,27,29,39–52] Extremely sterically hindered acenes,[53–56] i.e., twisted acenes and heterocenes,[57–61] where one or more carbons of the acenes are replaced by heteroatoms, have also been introduced to address the stability issue. In recent years, offline π-extension, including cyclopentannulation (A)[62–70] and benzo-annulation[71–74] (B, C, and D) has emerged as an effective strategy to stabilize acenes (Figure 1a). Five-membered rings have non-alternant electronic structures and can serve as electron acceptors.[62,64–66] Due to these features, incorporation of a 5-membered ring into acenes is expected to not only further stabilize the electron-rich acenes but also bring in unprecedented novel properties. However, almost all reported cyclopentannulation on acenes is at the peri-positions,[62–70] which gives rise to electronic and photophysical properties non-typical of acenes. As a result, singlet fission has not been reported for cyclopentannulated acenes. In this work, we introduce a new approach to incorporate a five-membered ring into acenes through linear fusion of acenaphthylene to pentacene (Figure 1b). The acenaphthylene-fused pentacenes, featuring more linearly cata-fused rings, showed stability comparable to or better than their pentacene analogues. Crucially, it maintained its optical and photophysical properties, achieving an efficient, ultrafast singlet fission with a triplet quantum yield of approximately 158% in thin films.

Acenaphthylene is composed of a naphthalene and an ethylene bridge located at a fused 5-membered ring. Although having 12 π-electrons, acenaphthylene is overall aromatic with the five-membered ring showing only slight anti-aromaticity.[75–78] Our goal is two-fold: First, we investigate the impact of acenaphthylene on the stability of the resulting molecular system. Second, we investigate whether the resulting molecular system retains the photophysical properties of acene necessary to facilitate singlet fission. In addition, the incorporation of an acenaphthylene unit into pentacene will introduce asymmetry into the resulting acenes, a factor that has rarely been investigated for crystal packing. Herein, the impact of the acenaphthylene unit on the optical properties, stability, crystal packing, and ultrafast processes of a linearly modified acene (**Ace-PCSi**) was investigated using steady-state and femtosecond time-resolved transient absorption spectroscopies and X-ray crystallography. Our studies have unveiled new photoinduced ultrafast carrier dynamics involving underlying triplet states in **Ace-PCSi** for singlet fission. Time-resolved electron paramagnetic resonance (TREPR) spectroscopy was used to elucidate the spin-state evolution during the occurrence of singlet fission. Favourable energetics of the associated excited-states and strong intermolecular vibronic interactions facilitating such efficient singlet-triplet evolutions have also been tracked synergically through DFT calculations and X-ray crystallography of the new acene.

Results and Discussion

Design and Synthesis of Acenaphthylene-Fused Pentacene

To synthesize a linearly acenaphthylene extended acene, we planned to first prepare fluoranthene-8,9-dicarbaldehyde **2**. Fluoranthene-8,9-dicarbaldehyde **2** has not been reported in

Open Access Article. Published on 02 June 2026. Downloaded on 6/4/2026 9:29:30 PM. This article is licensed under a Creative Commons Attribution 3.0 Unported Licence.

Chemical Science Accepted Manuscript

This journal is © The Royal Society of Chemistry 20xx

View Article Online
DOI: 10.1039/D5SC08246C

Open Access Article. Published on 02 June 2026. Downloaded on 6/4/2026 9:29:30 PM.
This article is licensed under a Creative Commons Attribution 3.0 Unported Licence.

Chemical Science Accepted Manuscript

the literature, and therefore, a synthetic method must be developed to access **2**. We decided to attempt a Heck reaction-based cascade reaction on 1,2-dibromoacenaphthylene **1** (Scheme 1), which was developed in our laboratory to access functionalized benzoporphyrins.[79] Acenaphthylene is a useful building block for π-electron functional materials.[77,78] The development of a new synthetic strategy to functionalize acenaphthylene will open new doors for functional materials.

The Heck reaction-based cascade reaction, which involves a Heck reaction, a 6 π-cyclization, and aromatization (Scheme 1), appears to be an ideal approach to serve this purpose. The Heck-based cascade reaction was first attempted with acrolein and 1,2-dibromoacenaphthylene **1**[80] through optimizing established conditions. However, a complex mixture always resulted, likely due to the unstable nature of both **1** and acrolein. Fortunately, the Heck-based cascade reaction was successfully carried out under colloidal Heck conditions[81,82] with acrolein diethyl acetal as the alkene. In the colloidal Heck conditions, tetrabutylammonium acetate was used as a phase transfer reagent, potassium chloride as an inorganic additive to assist in the colloid formation, potassium carbonate as a base, and palladium acetate as the Heck catalyst. It was observed that when water was present, the reaction would not undergo total oxidation, and the unoxidized fluoranthene-8,9-dicarbaldehyde was the major product. The addition of activated 4Å molecular sieves removed water from the solution and facilitated the reaction. After 72 hours, the reaction crude was hydrolyzed with diluted HCl to generate the desired fluoranthene-8,9-dicarbaldehyde **2** in a single step with 30% yield.

Fluoranthene-8,9-dicarbaldehyde **2** was treated with 2,3-dihydroanthracene-1,4-dione **4**, which was obtained through the reduction of commercially available anthracene-1,4-dione **3**, under basic conditions through double aldol condensation to give **Ace-PQ**. It is notable that 2,3-dihydroanthracene-1,4-dione **4** is highly sensitive to air; the reduction and the subsequent aldol condensation reactions were carried out under air-free conditions. Despite Ace-PQ being completely insoluble in all common solvents, Ace-PQ smoothly underwent an addition reaction with acetylide, followed by reductive aromatization using stannous chloride and acetic acid to generate the acenaphthylene-fused pentacene **Ace-PCPh** and **Ace-PCSi**. For comparison purposes, pentacene **BEPPh** and **BEPSi** were also prepared using a similar approach. **Ace-PCPh** was originally prepared first. However, attempts to prepare thin films using **Ace-PCPh** failed due to its low solubility. We then switched to the 6,13-bis(triisopropylsilylethynyl) (TIPS) substituted **Ace-PCSi**, as the TIPS-substituents provide better solubility. Thin films needed for the singlet fission study were successfully obtained using this derivative.

Optical Properties and DFT Calculation

The optical properties of **Ace-PCPh** and **Ace-PCSi** were measured by UV-Vis absorption and fluorescence spectroscopies (Figure 2 and Figure S1&2). Unlike the peri- and peri-/cata-annulated acenes (Figure 1, A, B, and C),[62–67] the UV-

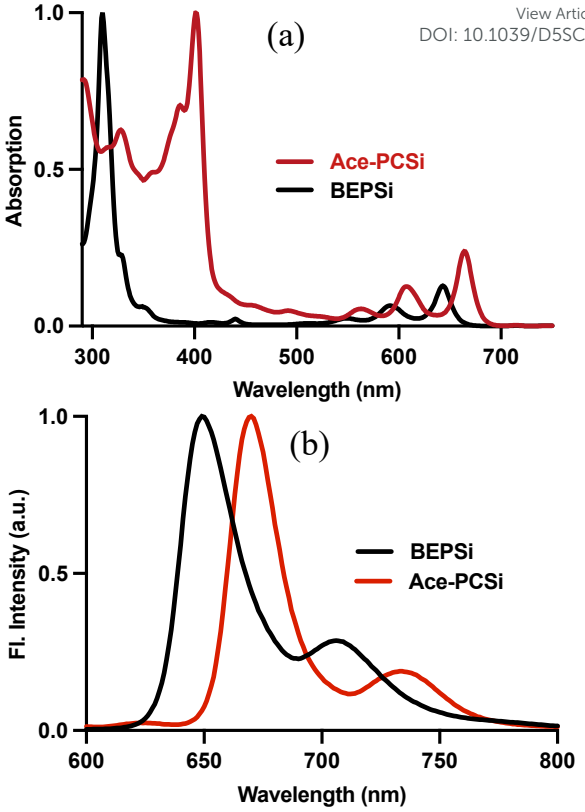

Figure 2. Normalized (a) UV-Vis absorption spectra, (b) Fluorescence spectra of **Ace-PCSi** and **BEPSi** in toluene. Excitation at 457 nm for **Ace-PCSi** and 440 nm for **BEPSi**.

Vis absorption spectra of both **Ace-PCPh** and **Ace-PCSi** displayed typical characteristic α, β and p bands of acenes, which were found at 402, 496, 678 nm and 401, 493, 664 nm, respectively. It is notable that the β bands of **Ace-PCPh** and **Ace-PCSi** showed the largest bathochromic shift relative to those of their pentacene analogues by ~45 and 92 nm, respectively. The α and p bands were also significantly red-shifted, highlighting the effect of π-extension. Consistent with the absorption results, the emission bands of **Ace-PCSi** are red-shifted compared to those of **BEPSi**. Notably, considering the lowest energy absorption and highest energy emission peaks at ~664 and 678 nm, respectively, the singlet state (S_1) energy for **Ace-PCSi** could be calculated as ~1.86 eV. Its triplet state (T_1) appears at ~0.80 eV based on phosphorescence data (Figure S3 in ESI). Interestingly, more than twice as the energy for the S_1 over T_1 state indicates a bright prospect of **Ace-PCSi** towards efficient singlet fission.[51,52] Both the HOMOs and LUMOs of **Ace-PCSi** and **Ace-PCPh** from DFT calculations (Figure S12 &13 in ESI) are centered at the pentacene unit with only slight involvement of the acenaphthylene unit, which explains their characteristic absorption bands on the UV-Vis absorption spectra. The HOMO shows slightly greater participation of the acenaphthylene unit than the LUMO. The HOMO energy level of **Ace-PCSi** is elevated to that of **BEPSi,** and the LUMO is slightly lowered (Figure S14 in ESI). As a result, the calculated HOMO-LUMO energy gap of **Ace-PCSi** (1.90 eV) is narrower than that of pentacene **BEPSi** (1.93 eV), which agrees with the red-shifted vibronically structured

View Article Online
DOI: 10.1039/D5SC02016C

Open Access Article. Published on 02 June 2026. Downloaded on 6/4/2026 9:29:30 PM.
This article is licensed under a Creative Commons Attribution 3.0 Unported Licence.

(finger structure) UV-vis spectra of **Ace-PCSi** and the optical band gaps (1.80 eV and 1.85 eV for **Ace-PCSi** and **BEPSi,** respectively, Table S1 in ESI). On the other hand, the acenaphthylene unit heavily contributes to the HOMO-1 and LUMO+1 of **Ace-PCSi** and **Ace-PCPh**. The energy level of the LUMO+1 is significantly lowered, and the HOMO-1 is significantly elevated compared to those of **BEPSi** and **BEPPh**, which is reflected by the largely red-shifted β bands on the UV-Vis spectra of **Ace-PCSi** and **Ace-PCPh.** The fluorescence spectra of **Ace-PCSi** displayed two emission bands at 670 nm and 734 nm, which are significantly red-shifted relative to those of **BEPSi**, consistent with the steady-state absorption and computational data. It is notable that **Ace-PCSi** has a longer fluorescence lifetime than **BEPSi**, with measurements of 15.3 ns (air) and 20.4 ns (argon), versus 12.6 ns and 17.3 ns, respectively (Figures S11 in ESI). To further understand the electronic transitions, we used TD-DFT calculations to assign the absorption bands of **BEP-Si** and **Ace-PCSi** (Figures S4 & 5 in ESI).

The photostability of **Ace-PCPh**, **BEPPh, Ace-PCSi**, and **BEPSi** was monitored by UV-vis absorption spectroscopy in 0.01 mM benzene solution under constant exposure to light and air (Figures S6-10 in ESI). The half-life was determined to be 45 h (**Ace-PCPh**), 33 h (**BEPPh)**, 688 min **(Ace-PCSi**), and 795 min (**BEPSi**). Overall, the acenaphthylene-fused pentacenes exhibited superior or comparable stability to their pentacene analogues. **Ace-PCPh** and **Ace-PCSi** are linearly π-extended and can be deemed as longer acenes than pentacene. The stability results are surprising given the higher HOMO energy levels and narrower HOMO-LUMO gaps, which typically suggest lower stability. The data in this section highlight how the addition of an acenaphthylene unit perturbs the electronic characteristics of acenes.

Single Crystal X-ray Crystallography

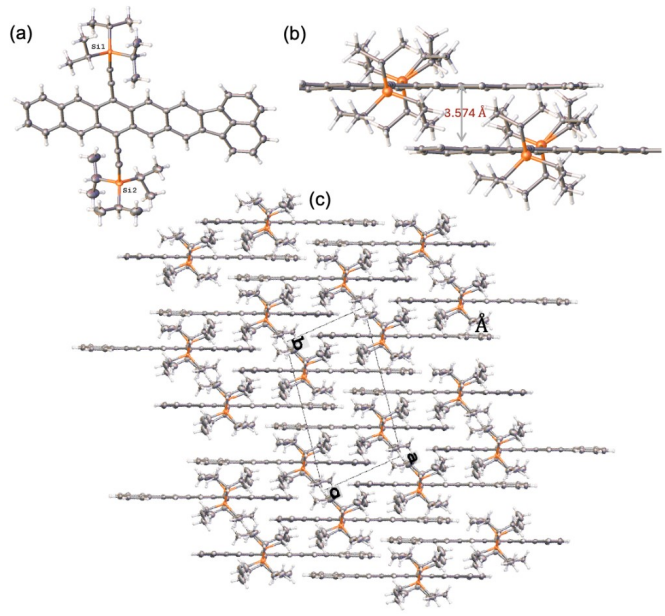

Figure 3. **Ace-PCSi**: (a) X-ray crystal structure (b) Crystal packing mode of two adjacent molecules (c) A packing motif.

Single crystal structures of **Ace-PCSi** and **BEPPh** were resolved (Figure 3 and Figures S32-34 in ESI, CCDC 2450036 and 2450035, respectively). **Ace-PCSi** adopts a strictly planar yet asymmetrical geometry. Notably, an asymmetric pentacene reported by the Anthony group adopts a herringbone packing.[83] In sharp contrast, the **Ace-PCSi** assumes a brick wall packing pattern with significant overlap of the adjacent molecules (Figure 3b), highlighting the effect of the acenaphthalene. This is intriguing considering the asymmetric structure of **Ace-PCSi**. The herringbone packing results in different layered structures with both face-to-edge and edge-to-edge modes. The brick wall packing pattern is expected to facilitate long-range intermolecular interactions through maintaining substantial face-to-face overlap. The interplanar distance between two closest **Ace-PCSi** molecules is 3.574 Å. Notably, the single-crystal structure of **BEPPh** was also obtained, revealing a herringbone packing motif similar to that of unsubstituted pentacene.[84-88]

Transient Absorption Spectroscopy

The favorable packing patterns with closer π-stacked systems in the solid-state hint that there could be a strong intermolecular coupling between two adjacent **Ace-PCSi**, which is clearly reflected from its red-shifted and relatively broad vibrational progression absorption bands in the thin film (Figure 4a). In contrast to the solution, the broad and red-shifted vibrational bands in the solid state suggest a J-aggregate-type spectrum[89,90] of **Ace-PCSi** with strong intermolecular vibronic coupling, which has also been confirmed with Powder X-Ray Diffractometry (PXRD) conducted for the thin film (Figure S35 in ESI). Additionally, the excited-state DFT calculation also provides an excited-state energy of S_1 and T_1 states at 1.90 and 0.63 eV, respectively, demonstrating $E(S_1)>2E(T_1)$ and thus satisfying the energy requirement for singlet fission (Figure S19 in ESI).[91–94] Prompted by these initial prerequisites, we then tried to disentangle the interplay of excited-state events as photoinduced singlet fission using ultrafast transient absorption (TA) spectroscopy in thin films as they closely replicate the operational conditions (i.e. solid-state environment) under which solar energy absorbers function in contemporary light-conversion applications. The TA spectroscopic data were specifically collected from the **Ace-PCSi** thin films (thickness of ~10 nm) using 630 nm excitation. The thickness and morphology of the films were measured with AFM/ Ellipsometry and PXRD, respectively (Figures S36 and S37 in ESI). Since the efficiency of singlet fission greatly depends on competitive parasitic non-/radiative deactivations with effective generation of correlated triplet pairs in the ultrafast time domain,[93] Figure 4b thus summarizes the early-time (up to ~1 ps) spectral behavior of the **Ace-PCSi** thin film in the visible and near infrared (NIR) window. Significant spectral evolution is observed in the early stages of both regions. For example, the excited state absorption (ESA) in visible exhibits continuously evolving signals at ~470-500 nm before ~500 fs and finally peaks at ~550-560 nm around ~0.8-1 ps (Figure 4b). A similar spectral signature in initial delay for TIPS-pentacene was attributed to the ESA feature of states with different

Chemical Science Accepted Manuscript

This journal is © The Royal Society of Chemistry 20xx

View Article Online
DOI: 10.1039/D5SC08246C

Open Access Article. Published on 02 June 2026. Downloaded on 6/4/2026 9:29:30 PM.
This article is licensed under a Creative Commons Attribution 3.0 Unported Licence.

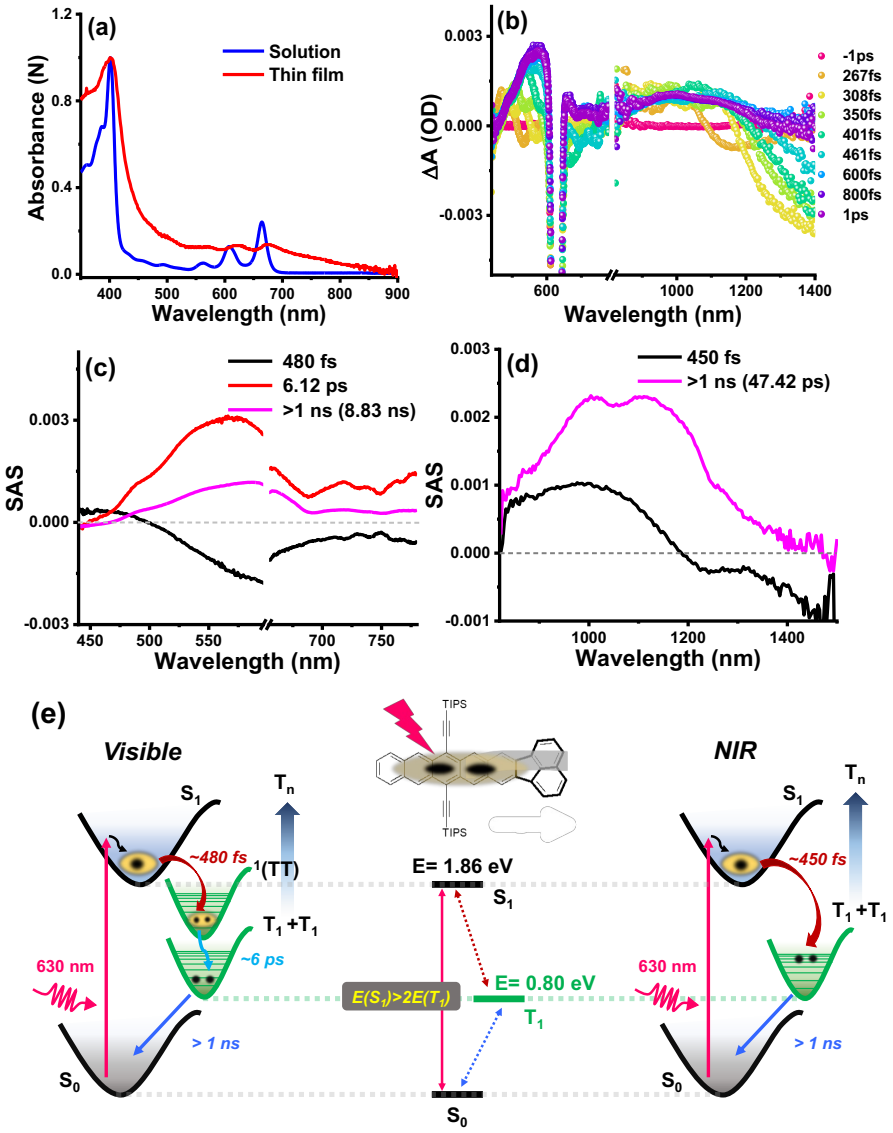

Figure 4. (a) Ground state absorption feature of **Ace-PCSi** in toluene and spin-coated thin films. (b) fs-TA spectral evolutions at the indicated probe delays in the early time scale. (c and d) SAS was achieved after the GTA of the fs-TA data in the visible and NIR windows, respectively. The SAS representing 47.42 ps ideally possesses a time constant of 3.91 ns (>1 ns) upon complete fitting to the offset. (e) A schematic representation of the excited-state dynamics and energetics of different states involved in the singlet fission of **Ace-PCSi.** For simplicity, the potential energy surface of one T_1 state is shown after the first step of singlet fission.

multiplicity by Ramanan et al, vis-à-vis singlet fission mediated S_1 to T_1 conversion.[95] The early time short wavelength (<500 nm) spectral features thus can be assigned to ESA related to singlets ($S_1 \rightarrow S_n$), which subsequently undergoes an ultrafast conversion into triplets, leading to triplet ESA ($T_1 \rightarrow T_n$) at ~550-560 nm. Such an ultrafast transition of singlet into triplet is not surprising, as efficient singlet fission is believed to proceed via a spin-conserved (and thus faster) intermediate, known as correlated triplet pair ^{1}(TT).[96–99] Similarly, in the NIR, a relatively narrow ESA appearing at ~850-1100 nm before ~500 fs quickly evolves into a broader absorption band by <1 ps, covering almost the entire detectable NIR window (Figure 4b). These synergistically evolved ultrafast spectral transitions in NIR are also consistent with those observed in the visible and are thus attributed to the characteristic conversion of the directly formed singlets into triplets following photoexcitation.[100–102] Although a comparison of similar experiments done in dilute solution and compact films are trivial, the relative position of ESAs obtained upon 630 nm photoexcitation of 0.01 mM **Ace-PCSi** in toluene at ~475 and 850-1100 nm, respectively in the visible and NIR related to singlet states, is found to be closely comparable to that observed in thin film of the compound (Figures S20 in ESI). Note that poor intermolecular interaction between Ace-PCSi in such a dilute medium constitutes spectral features predominantly of the singlet states even after >2 ns, and in stark contrast to that of the solid thin films. Consistent with this, rubrene populates its singlet excited state in solution predominantly due to inefficient intersystem crossing (a

Chemical Science Accepted Manuscript

View Article Online
DOI: 10.1039/D5SC09246G

Open Access Article. Published on 02 June 2026. Downloaded on 6/4/2026 9:29:30 PM. This article is licensed under a Creative Commons Attribution 3.0 Unported Licence.

radiationless unimolecular process that competes with singlet fission), whereas in the solid single-crystalline state, triplet absorption arising from efficient singlet fission dominates.[116] These observations underscore the decisive role of intermolecular electronic coupling in enabling exothermic singlet fission in the solid state of polyaromatic hydrocarbons. The intermediate ^{1}(TT) state formed latest by 1 ps upon photoexcitation and then subsequently makes spectrally silent relaxation into independent triplets (T_1) and thereby no new spectral signature appears in a longer time window for the triplets before deactivation to the ground state (S_0) (Figure S21 in ESI).

Insight into the spectral features of the involved species from the overlapping TA signals, along with their associated time constants, was further assessed by performing global target analysis (GTA) of the visible and NIR data datasets independently; the results are summarized in Figures 4c and 4d, respectively. Based on previous reports on pentacene derivatives, a sequential relaxation model has been introduced on GTA to deconvolute spectral information of the photoexcited state processes in **Ace-PCSi** thin film.[100–103] The first species associated spectra (SAS) in the visible appear as a broad spectrum with significant contribution in the bluer side (~450-490 nm) of the region with no-to-negative contribution after ~500 nm, indicating S_1 state forms directly after photoexcitation and decays with a time constant of ~480 fs (Figure 4c). It is notable that the time constant for S_1 state decay of **Ace-PCSi** is significantly longer than that reported for pentacene and its derivatives (50-200 fs).[100,103] Although acenaphthylene is overall aromatic, the five-membered ring possesses slight anti-aromaticity. We suspect that upon excitation, it becomes aromatic in the excited state according to Baird's rule, and thus, a more stable Sπ state with a prolonged lifetime was observed.[104–108] However, NICS analysis reveals slight antiaromaticity of the 5-membered ring and decreased aromaticity of the adjacent benzene ring in ^{0}S, ^{1}S and ^{1}T states (Table S2 in ESI). The blue end of the other two species is much less pronounced, though. Instead, a stronger and more intense ESA feature associated with ^{1}(TT) (red) emerges, centered after 550 nm, with a lifetime of approximately 6.12 ps. It is important to note that the involvement of two different types of interconvertible correlated triplet-pair intermediates (spatially interacting and noninteracting) on a few ~ps timescales had been previously proposed during singlet fission of pentacene derivatives.[97,99,103] Triplet energy transfer, leading to a change in excitonic interactions and occurring on a ~ps time frame, was reported to be key in facilitating such interconversion of crystalline acenes.[99,109,110] Notably, in our case, the ~6.12 ps time constant associated with this second, i.e., correlated 1(TT) state, is closely comparable with the triplet energy transfer rate in crystalline pentacenes, and therefore participation of two spectrally identical and spatially interconvertible triplet pair intermediates can't be ruled out. The third SAS, representing the independent T_1 states with almost similar spectral features to those of correlated triplet pairs, finally decays to the ground S_0 state with a time constant of >1 ns.[98,100–102]

Unlike visible, the assessment of S_1/T_1 spectral characteristics in NIR for pentacene (and its derivatives) has historically been counterintuitive, with some reports claiming to be free of any S_1 spectral contribution,[111,112] while others demonstrated an overlapping $S_1 \rightarrow T_1$ signal in this region.[100,113] However, here the calculated sub-unity energy for the T_1 state promises to exhibit signature absorption in the NIR due to the transition between triplet energy states of **Ace-PCSi**. That being said, owing to the ultrafast early time events of S_1 to correlated triplet pair formation in the visible, GTA in NIR has been carried out, taking the initial (up to 50 ps) spectral evolutions into account so that minute spectroscopic information for any such transitions in a shorter time domain is not overlooked. Interestingly, a two-component GTA fitting in the NIR satisfactorily describes the excited-state photoevents in **Ace-PCSi** (Figure 4d), whereas a three-component fitting, even over a longer time window (like that in visible), does not substantially improve the NIR fitting quality (Figure S22 in ESI). It indicates that photoinduced processes, particularly in the early delay at NIR, are presumably faster than those in the visible region. This is not surprising as the time constant associated with triplet pair formation in acenes is usually in the order of a few hundred fs and becomes relatively faster with gradual red-shift (visible-to-NIR) of excitonic singlet absorption owing to modulation in driving force of this step,[101,102], and also undergoes a different relaxation pathway in the NIR.[100] The first component, exhibiting a broad spectrum up to ~1180 nm, decays with a time constant of ~450 fs (comparable to that in the visible) and quickly evolves into an even broader spectrum with a lifetime of ~47.42 ps, spanning nearly the entire NIR window, corresponding respectively to the S_1 and T_1 states of **Ace-PCSi**. Notably, since GTA is performed using only a limited initial time window, the second component representing T_1 ideally possesses a time constant of >1 ns upon complete fitting to the offset; however, a value of ~3.91 ns is obtained. Needless to mention, this longer decay time for T_1 before spin-forbidden recombination to the ground state is particularly desirable, as this long-excited state provides a better larger time window to effectively extract the photogenerated charge carriers for solar energy conversions. Interestingly, the amplitude of the deconvoluted S_1 signals are found to be much less than that of the T_1 states in both the NIR and visible regions, indicating transients undergoing triplet absorption are more than initially populated singlets and thereby suggests the linearly cyclopentannulated acenes **Ace-PCSi** can indeed undergo an efficient singlet fission mediated multiexciton formation in ultrafast time regime, a phenomenon that has not been seen in this class of acenes. Consequently, a pronounced singlet fission is also exemplified by a calculated triplet yield of ~158% (see details in ESI), in line with the spectral data, and indicates a lesser extent of possible energy-wasting competitive processes. However, although singlet fission is efficient and occurs on a sub-ps timescale, a 158% triplet yield suggests the presence of unavoidable deactivation processes. Radiative (fluorescence) and non-radiative events from S_1 are expected to be operative

Chemical Science Accepted Manuscript

This journal is © The Royal Society of Chemistry 20xx

View Article Online
DOI: 10.1039/D5SC08246C

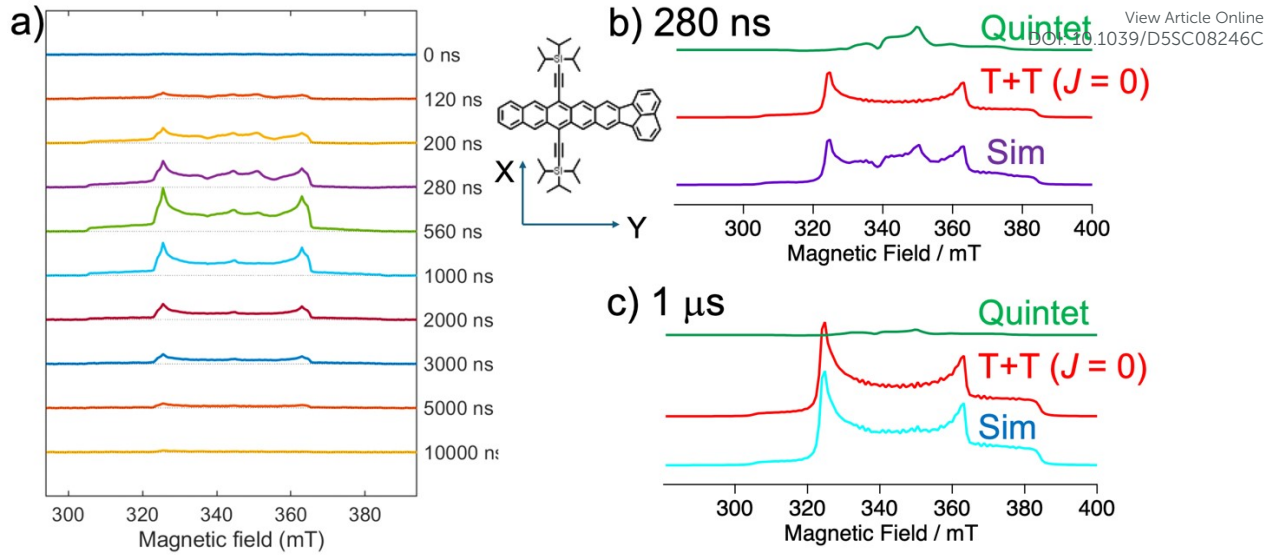

Figure 5. (a) Delay time dependence of the TREPR spectrum obtained by 532 nm laser irradiation of **Ace-PCSi** film at 80 K. The film was prepared by drop-casting a 1 mM toluene solution of 0.2 mL onto a cover glass. Microwave frequency is 9663.79 MHz. (b,c) Simulations of the TREPR spectra for the two different time regions by summations of the computed quintet and T+T hyperpolarized EPR spectra.

at early times with the addition of other deactivation pathways (to S_0) originating from the intermediate and/or final excited states, particularly as time elapses. However, these have historically been difficult to trace for pentacene derivatives.[103] Importantly, triplet-triplet annihilation mediated deactivation is unlikely here due to $E(T_2)>2E(T_1)$ of **Ace-PCSi** accessed from excited state DFT studies (T_1= 0.63 and T_2= 2.81 eV). **Ace-PCSi**, although it possesses S_1/T_1 spectral signatures in the NIR, a clear distinction between the two states, both in terms of spectral and kinetic information, is evident, particularly after the GTA fittings.[100–102] Notably, a relatively faster decay of S_1 state for the formation of triplet in the NIR over the visible suggests that two different ultrafast channels are associated with the ESAs from T_1 in the visible and NIR and thus likely probe different transitions involving different initial vibrational levels on the excited T_1 potential energy surface (Figure 4e). For example, while the longer formation time of the correlated triplet pair (i.e. decay of S_1) corresponds to the association of deep (lower) vibrational levels on the triplet potential surface in visible, the same in the NIR presumably originates from shallow (higher) vibrational levels (Figure 4e). Furthermore, the absence of a reliable intermediate state with a lifetime of a few ps in NIR indicates higher lying triplets (T_n) decay to the ground state of **Ace-PCSi** following different pathways in these two spectral regions.[100–102] It is, however, expected that, due to the involvement of underlying triplet states in **Ace-PCSi** following singlet fission, magnetic-field-dependent photoinduced ultrafast carrier dynamics may open a new avenue for elucidating uncharacterized intermediates and their spectroscopic fingerprints. This work, however, specifically unveils that linearly fused cata-π-extended pentacenes can indeed be a solution over peri-annulated chromophores to not only improve the overall stability of acene derivatives but also to retain their intrinsic optical properties, including the coveted singlet fission characteristics with a triplet yield of 158% in photovoltaics. Note that this value is considerably high and, in some cases, even better than common monomeric exothermic and endothermic acenes (Table S3). Furthermore, a slightly higher triplet energy of **Ace-PCSi** than standard TIPS-Pentacene (0.80 vs. 0.78 eV)[114,115] and its π-extended architecture contribute to a relatively broad and red-shifted absorption over TIPS-Pentacene analog (Figures 2a),[113] making **Ace-PCSi** an even better independent solar light absorber and holds promise to be incorporated in tandem with silicon for solar energy conversion devices. Finally, this new cata-π-extension approach is found to hold great promise over the previously developed peri-modulations in both the current toolset of synthetic protocols for stable acenes and retaining explicit photophysical characteristics for technological advancements.

Time-Resolved Electron Paramagnetic Resonance Spectroscopy

To further elucidate the nature of the triplet pairs and their dynamics, time-resolved electron paramagnetic resonance (TREPR) spectroscopy was employed for a neat **Ace-PCSi** thin film prepared with a drop cast method from a 1 mM toluene solution. Figure 5 shows X-band TREPR spectra obtained by 532 nm laser irradiation of this film at 80 K. The microwave absorptive (A) hyperpolarized spectra were observed around a g-value of 2.003 from the microwave frequency of 9663.78 MHz, denoting that the fine structure from the triplet species is observed as a Pake pattern from D = 1050 MHz and E = 15 MHz in Table S4. In addition to the strong large fine structure exhibiting a 40 mT peak splitting, weak spike signals overlap around 330 mT and 350 mT at the delay times shorter than 1000 ns. This emission(E)/absorption(A) overlapping polarization is assigned to the quintet state of the strongly coupled triplet-pair.[117]

To understand the time variation of the spectra, we performed a spin-quantum model calculation of the triple pairs

Open Access Article. Published on 02 June 2026. Downloaded on 6/4/2026 9:29:30 PM.
This article is licensed under a Creative Commons Attribution 3.0 Unported Licence.

Chemical Science Accepted Manuscript

View Article Online
DOI: 10.1039/D5SC08246G

with considering the effects of the spin Hamiltonian on the exciton motion in the strongly coupled TTs (^{1}TT, ^{3}TT and ^{5}TT) composed of TT_1 and TT_2 states, and in the weakly-coupled triplet pair containing the nine coupled superpositions of the basis spin functions of the diabatic $^1(T_1+T_1)$, $^3(T_1+T_1)$ and $^5(T_1+T_1)$ characters in the presence of the exchange interaction (J) and of the external magnetic field, as reported previously.[118, 119] Table S4 summarizes the EPR and kinetic parameters to compute the hyperpolarized spectra of the quintet TT state and the separated T+T state at the delay times of 280 ns and 1 μs in b) and c) of Figure 5, respectively. The absorptive feature of the spin polarization is explained by the disordered sub-nanosecond conformation dynamics of the triplet exciton within the triplet pairs. This indicates that the exciton migration of the singlet-fission-born triplets is undergoing the exciton migration within the pair for the singlet-quintet spin conversions to the spin sublevels (m_S) of $^5TT_{m_S\leq 0}$ in the presence of the magnetic field. Summations of the quintet and T+T spectra are shown as the simulated spectra in Figure 5b and 5c, those of which explain the experimental data in a).

From Table S4, the singlet-precursor (^{1}TT) spin interconversions occur to the quintet with the spin sublevels in $^5TT_{m_S\leq 0}$ in the presence of the magnetic field via the TT_2 state, in which the T_B triplet in the T_AT_B multiexciton takes a dihedral rotation by β = -76 degrees from the TT_1 state at the activation to weaken the exchange coupling (-11 GHz). This activation motion in the present neat thin-film sample is relevant to the triplet-exciton diffusion within the disordered solid-state environment from the strongly coupled parallel TT_1 conformation to cause the TT_2 state with the distorted triplet-pair conformation. At 1 μs, the absence and the presence of the of the quintet species and the absorptive individual triplet polarization, respectively, are explained by the preferential T+T dissociation ($k_{Diss} > k_{Back}$) from the quintet species in Figure 5c. Overall, the quintet EPR and the subsequent T+T hyperpolarization signals are the consequences of the efficient intermolecular singlet fission in a molecularly ordered crystalline environment and subsequent triplet exciton migration in the disordered region in the drop cast film. In summary, the delay time dependence of the TREPR spectrum demonstrates that singlet-precursor spin interconversions to the quintet (^{5}TT) with specific spin sublevels occur from the strongly coupled triplet-pair (^{1}TT), followed by triplet exciton dissociation from ^{5}TT.

Conclusions

In conclusion, we have developed a new synthetic method to linearly fuse acenaphthylene, which contains a 5-membered ring, to pentacene. In sharp contrast to other acenes stabilized through cyclopentannulation and other π-extension, which display non-typical properties of acene and thus fail to undergo singlet fission, the acenaphtho[1,2-b]pentacenes **Ace-PCSi** and **Ace-PCPh** possess characteristic electronic and photophysical properties of acenes. The thin film formed from the **Ace-PCSi** demonstrated efficient singlet fission-mediated triplet multiexciton generation in the ultrafast time regime, with a triplet quantum yield of up to 158%. (TREPR) spectroscopy revealed the sequence of spin-state changes occurring during singlet fission, further confirming the formation of triplet pairs during singlet fission process. In particular, the observation of the normally elusive quintet (^{5}TT) state is notable. The impact of the acenaphthylene fusion to pentacene is further highlighted by a much longer S_1 state and fluorescence lifetime of **Ace-PCSi,** and by the clear identification of a singlet contribution to the NIR absorption range with pronounced distinction between the S_1 and T_1 states, which have not been observed in pentacene and its derivatives.

Despite having reduced HOMO-LUMO energy gaps and elevated HOMO energy levels, linearly elongated acenaphthylene-fused pentacenes exhibit stability similar to that of their pentacene counterparts. A favorable slip-stack columnar packing pattern has been discovered in the unsymmetrical acenaphtho[1,2-b]pentacene **Ace-PCSi**, representing a notable departure from the packing behavior of other unsymmetrical acenes. This work highlights that linear fusion of acenaphthylene to acene can serve as an effective strategy to stabilize acenes while improving their photophysical properties for singlet fission. The introduction of acenaphthylene-fused acenes extends the scope of materials that can undergo singlet fission, a field previously known for its scarcity of suitable materials. The information obtained from this work will also advance the basic knowledge in understanding 4n π electron systems.

Author contributions

H. W. and J. A. designed the project. J. A. and S. S. conducted the synthesis and characterization of the compounds. S. S and A. W. D carried out initial spectral studies of the compounds. S. D. designed and carried out the experiments for transient absorption spectroscopy and data analysis. S. T. and Y. K. designed and carried out the experiments for time-resolved electron paramagnetic resonance spectroscopy. S. S performed all the computations. V. N. N. collected the X-ray diffraction data and solved the crystal structures. S. S., T. P., and S. L. designed and conducted film preparation and measurements. All authors contributed to data analysis and manuscript writing.

Conflicts of interest

There are no conflicts to declare.

Data availability

Supporting data for this article, including experimental methods and characterization data, are provided in the supplementary information (SI).

Acknowledgements

This work was supported by the U.S. Department of Energy, Office of Science, Basic Energy Sciences under Award DE-

Open Access Article. Published on 02 June 2026. Downloaded on 6/4/2026 9:29:30 PM. This article is licensed under a Creative Commons Attribution 3.0 Unported Licence.

Chemical Science Accepted Manuscript

View Article Online
DOI: 10.1039/D5SC08240C

SC0016766. We acknowledge the National Science Foundation MRI Program (CHE-1726652) and the University of North Texas for supporting the acquisition of the Rigaku XtaLAB Synergy-S X-ray diffractometer. This work was partially supported by JSPS KAKENHI Grant Numbers of 24H00485, 25H00903) and Grant Nos. 25K22299, JST-CREST Program (JPMJCR23I6), and MEXT Quantum Leap Flagship Program, Japan (JPMXS0120330644). YK also thanks a support from Kobe University Strategic International Collaborative Research Grant (Type B Fostering Joint Research). We thank Dr. Francis D'Souza for helpful discussion and insightful suggestions.

Notes and references

1 J. E. Anthony, *Chem. Rev*, 2006, **106**, 5028–5048.
2 J. E. Anthony, *Angew. Chem. Int. Ed*, 2008, **47**, 452–483.
3 M. Watanabe, K.-Y. Chen, Y. J. Chang and T. J. Chow, *Acc. Chem. Res*, 2013, **46**, 1606–1615.
4 M. Ball, Y. Zhong, Y. Wu, C. Schenck, F. Ng, M. Steigerwald, S. Xiao and C. Nuckolls, *Acc. Chem. Res*, 2015, **48**, 267–276.
5 U. H. Bunz, *Acc. Chem. Res*, 2015, **48**, 1676–1686.
6 U. H. Bunz and J. U. Engelhart, *Chem. Eur. J*, 2016, **22**, 4680–4689.
7 J. L. Marshall, D. Lehnherr, B. D. Lindner and R. R. Tykwinski, *ChemPlusChem*, 2017, **82**, 967–1001.
8 X. K. Chen, D. Kim and J. L. Bredas, *Acc. Chem. Res*, 2018, **51**, 2215–2224.
9 A. Bedi and O. Gidron, *Acc. Chem. Res*, 2019, **52**, 2482–2490.
10 A. J. Lou and T. J. Marks, *Acc. Chem. Res*, 2019, **52**, 1428–1438.
11 T. Zhu and L. Huang, *J. Phys. Chem. Lett*, 2018, **9**, 6502–6510.
12 B. S. Basel, I. Papadopoulos, D. Thiel, R. Casillas, J. Zirzlmeier, T. Clark, D. M. Guldi and R. R. Tykwinski, *Trends in Chemistry*, 2019, **1**, 11–21.
13 J. Li, H. Cao, Z. Zhang, S. Liu and Y. Xia, *Photonics*, 2022, **9**, 689.
14 K. Miyata, F. S. Conrad-Burton, F. L. Geyer and X. Y. Zhu, *Chem. Rev*, 2019, **119**, 4261–4292.
15 C. Tonshoff and H. F. Bettinger, *Chem. Eur. J*, 2021, **27**, 3193–3212.
16 T. Wang, H. Liu, X. Wang, L. Tang, J. Zhou, X. Song, L. Lv, W. Chen, Y. Chen and X. Li, *J. Mater. Chem. A*, 2023, 8515–8539.
17 D. N. Congreve, J. Lee, N. J. Thompson, E. Hontz, S. R. Yost, P. D. Reusswig, M. E. Bahlke, S. Reineke, T. V. Voorhis and M. A. Baldo, *Science*, 2013, **340**, 334–337.
18 B. Daiber, K. Hoven, M. H. Futscher and B. Ehrler, *ACS Energy Lett*, 2021, **6**, 2800–2808.
19 M. K. Gish, N. A. Pace, G. Rumbles and J. C. Johnson, *J. Phys. Chem. C*, 2019, 3923–3934.
20 J. M. Luther and J. C. Johnson, *Nature*, 2019, **571**, 38–39.
21 L. M. Pazos-Outon, J. M. Lee, M. H. Futscher, A. Kirch, M. Tabachnyk, R. H. Friend and B. Ehrler, *ACS Energy Lett*, 2017, **2**, 476–480.
22 J. Xia, S. N. Sanders, W. Cheng, J. Z. Low, J. Liu, L. M. Campos and T. Sun, *Adv. Mater*, 2017, **29**, 1601652.
23 M. M. Payne, S. A. Odom, S. R. Parkin and J. E. Anthony, *Org. Lett.*, 2004, **6**, 3325–3328.
24 M. M. Payne, S. R. Parkin and J. E. Anthony, *J. Am. Chem. Soc*, 2005, **127**, 8028–8029.
25 D. -e Jiang and S. Dai, *J. Phys. Chem. A*, 2008, **112**, 332–335.
26 I. Kaur, N. N. Stein, R. P. Kopreski and G. P. Miller, *J. Am. Chem. Soc*, 2009, **131**, 3424–3425.
27 H. Qu and C. Chi, *Org. Lett*, 2010, **12**, 3360–3363.
28 C. Tonshoff and H. F. Bettinger, *Angew. Chem. Int. Ed*, 2010, **49**, 4125–4128.
29 S. S. Zade and M. Bendikov, *Angew. Chem. Int. Ed*, 2010, **49**, 4012–4015.
30 B. Purushothaman, S. R. Parkin, M. J. Kendrick, D. David, J. W. Ward, L. Yu, N. Stingelin, O. D. Jurchescu, O. Ostroverkhova and J. E. Anthony, *Chem Commun*, 2012, **48**, 8261–8263.
31 M. Watanabe, Y. J. Chang, S. W. Liu, T. H. Chao, K. Goto, M. M. Islam, C. H. Yuan, Y. T. Tao, T. Shinmyozu and T. J. Chow, *Nat. Chem*, 2012, **4**, 574–578.
32 R. Einholz and H. F. Bettinger, *Angew. Chem. Int. Ed*, 2013, **52**, 9818–9820.
33 Y. Yang, E. R. Davidson and W. Yang, *Proc. Natl. Acad. Sci. USA*, 2016, **113**, 5098–5107.
34 J. Kruger, F. Garcia, F. Eisenhut, D. Skidin, J. M. Alonso, E. Guitian, D. Perez, G. Cuniberti, F. Moresco and D. Pena, *Angew. Chem. Int. Ed*, 2017, **56**, 11945–11948.
35 S. Ray, S. Sharma, U. Salzner and S. Patil, *J. Phys. Chem. C*, 2017, **121**, 16088–16097.
36 R. G. Clevenger, B. Kumar, E. M. Menuey and K. V. Kilway, *Chem. Eur. J*, 2018, **24**, 3113–3116.
37 B. Shen, J. Tatchen, E. Sanchez-Garcia and H. F. Bettinger, *Angew. Chem. Int. Ed*, 2018, **57**, 10506–10509.
38 Y. Xiao, J. T. Mague, R. H. Schmehl, F. M. Haque and R. A. Pascal Jr, *Angew. Chem. Int. Ed*, 2019, 58 2831-2833.
39 J. E. Anthony, D. L. Eaton and S. R. Parkin, *Org. Lett*, 2002, 4,15-18.
40 Y. Sakamoto, T. Suzuki, M. Kobayashi, Y. Gao, Y. Fukai, Y. Inoue, F. Sato and S. Tokito, *J. Am. Chem. Soc*, 2004, **126**, 8138–8140.
41 A. L. Briseno, Q. Miao, M.-M. Ling, C. Reese, H. Meng, Z. Bao and F. Wudl, *J. Am. Chem. Soc*, 2006, **128**, 15576–15577.
42 Q. Miao, X. Chi, S. Xiao, R. Zeis, M. Lefenfeld, T. Siegrist, M. L. Steigerwald and C. Nuckolls, *J. Am. Chem. Soc*, 2006, **128**, 1340–1345.
43 I. Kaur, W. Jia, R. P. Kopreski, S. Selvarasah, M. R. Dokmeci and C. Pramanik, *J. Am. Chem. Soc*, 2008, **130**, 16274–16286.
44 B. H. Northrop, K. N. Houk and A. Maliakal, *Photochem. Photobiol. Sci*, 2008, **7**, 1463–1468.
45 Y.-F. Lim, Y. Shu, S. R. Parkin, J. E. Anthony and G. G. Malliaras, *J. Mater. Chem.*, 2009, **19**, 3049–3056.
46 S. Katsuta, D. Miyagi, H. Yamada, T. Okujima, S. Mori, K. -i Nakayama and H. Uno, *Org. Lett*, 2011, **13**, 1454–1457.
47 B. Purushothaman, M. Bruzek, S. R. Parkin, A. F. Miller and J. E. Anthony, *Angew. Chem. Int. Ed*, 2011, **50**, 7013–7017.
48 Q. Ye and C. Chi, *Chem. Mater*, 2014, **26**, 4046–4056.
49 J. Zhang, R. H. Pawle, T. E. Haas and S. W. Thomas, *Chem. Eur. J*, 3rd, **20**, 5880–5884.
50 S. R. Bheemireddy, P. C. Ubaldo, P. W. Rose, A. D. Finke, J. Zhuang, L. Wang and K. N. Plunkett, *Chem. Int. Ed*, 2015, 54,15762-15766.
51 M. Müller, L. Ahrens, V. Brosius, J. Freudenberg and U. H. F. Bunz, *J. Mater. Chem. C*, 2019, **7**, 14011–14034.
52 Q. Ye and C. Chi, *Chem. Mater*, 2014, **26**, 4046–4056.
53 A. Bedi and O. Gidron, *Acc. Chem. Res*, 2019, **52**, 2482–2490.
54 S. G. Davey, *Nat. Rev. Chem*, 2019, **3**, 67–67.
55 J. R. A. Pascal, *Chem. Rev*, 2006, **106**, 4809–4819.
56 A. Stanger, *Chemphyschem*, 2024, **25**, 202400128.
57 A. Borissov, Y. K. Maurya, L. Moshniaha, W. S. Wong, M. Zyla-Karwowska and M. Stepien, *Chem. Rev*, 2022, **122**, 565–788.
58 U. H. Bunz, J. U. Engelhart, B. D. Lindner and M. Schaffroth, *Angew. Chem. Int. Ed*, 2013, **52**, 3810–3821.
59 F. Kang, J. Yang and Q. Zhang, *J. Mater. Chem. C*, 2022, **10**, 2475–2493.
60 A. Mishra, *Energy Environ. Sci*, 2020, **13**, 4738–4793.
61 Q. Xiao-Ni, L.-R. Dang, W.-J. Qu, Y.-M. Zhang, H. Yao, Q. Lin and T.-B. Wei, *J. Mater. Chem. C*, 2020, **8**, 11308–11339.
62 S. R. Bheemireddy, P. C. Ubaldo, P. W. Rose, A. D. Finke, J. Zhuang, L. Wang and K. N. Plunkett, *Angew. Chem. Int. Ed*, 2015, **54**, 15762–15766.
63 G. Dai, J. Chang, J. Luo, S. Dong, N. Aratani, B. Zheng, K. W. Huang, H. Yamada and C. Chi, *Angew. Chem. Int. Ed*, 2016, **55**, 2693–2696.

Open Access Article. Published on 02 June 2026. Downloaded on 6/4/2026 9:29:30 PM.
This article is licensed under a Creative Commons Attribution 3.0 Unported Licence.

Chemical Science Accepted Manuscript

View Article Online
DOI: 10.1039/D5SC08246C

64 Y. Du, H. B. Lovell, F. Lirette, J. F. Morin and K. N. Plunkett, *J. Org. Chem*, 2021, **86**, 1456–1461.
65 P. H. Jacobse, M. C. Daugherty, K. N. Cernevics, Z. Wang, R. D. McCurdy, O. V. Yazyev, F. R. Fischer and M. F. Crommie, *ACS Nano*, 2023, **17**, 24901–24909.
66 A. N. Lakshminarayana, J. Chang, J. Luo, B. Zheng, K. W. Huang and C. Chi, *Chem. Commun*, 2015, **51**, 3604–3607.
67 X. Xiao and T. R. Hoye, *Nat. Chem*, 2018, **10**, 838–844.
68 R. Heckershoff, S. Maier, T. Wurm, P. Biegger, K. Brodner, P. Kramer, M. T. Hoffmann, L. Eberle, J. Stein, F. Rominger, M. Rudolph, J. Freudenberg, A. Dreuw, A. S. K. Hashmi and U. H. F. Bunz, *Chem. Eur. J*, 2022, **28**, 202104203.
69 S. Maier, R. Heckershoff, N. Hippchen, K. Brodner, F. Rominger, J. Freudenberg, A. S. K. Hashmi and U. H. F. Bunz, *Chem. Eur. J*, 2022, **28**, 202201842.
70 S. Maier, N. Hippchen, F. Jester, M. Dodds, M. Weber, L. Skarjan, F. Rominger, J. Freudenberg and U. H. F. Bunz, *Angew. Chem. Int. Ed*, 2023, **62**, 202214031.
71 V. M. Nichols, K. Broch, F. Schreiber and C. J. Bardeen, *J. Physic. Chem. C*, 2015, **119**, 12856–12864.
72 E. C. Rudiger, M. Muller, S. Koser, F. Rominger, J. Freudenberg and U. H. F. Bunz, *Chem. Eur. J*, 2018, **24**, 1036–1040.
73 W. Yang, J. Monteiro, A. Bettencourt-Dias, V. J. Catalano and W. A. Chalifoux, *Chem. Eur. J*, 2019, **25**, 1441–1445.
74 G. Zhang, F. Rominger, U. Zschieschang, H. Klauk and M. Mastalerz, *Chem. Eur. J*, 2016, **22**, 14840–14845.
75 P. Schleyer, C. Maerker, A. Dransfeld, H. Jiao and Njr. Hommes, *J. Am. Chem. Soc*, 1996, **118**, 6317–6318.
76 D. Liu, T. F. Liu, Y. P. Chen, L. Zou, D. Feng, K. Wang, Q. Zhang, S. Yuan, C. Zhong and H. C. Zhou, *Mechanistic Studies, and Potential Applications" J. Am. Chem. Soc*, 2015, **137**, 7740–7746.
77 Y.-H. Liu and D. F. Perepichka, *J. Mater. Chem. C*, 2021, **9**, 12448–12461.
78 Z. Wang, Q. Peng, X. Huang, Q. Ma, J. Shao and Q. Shen, *Dyes Pigm*, 2021, **185**, 108877.
79 R. Deshpande, L. Jiang, G. Schmidt, J. Rakovan, X. Wang, K. Wheeler and H. Wang, *Org. Lett*, 2009, **11**, 4251–4253.
80 B. Yuan, J. Zhuang, K. M. Kirmess, C. N. Bridgmohan, A. C. Whalley, L. Wang and K. N. Plunkett, *J. Org. Chem*, 2016, **81**, 8312–8318.
81 M. Belier, H. Fischer, K. Kiihlein, C.-P. Reisinger and W. A. Herrmarm, *J. Organomet. Chem*, 1996, **520**, 257–259.
82 S. Klingelhöfer, W. Heitz, A. Greiner, S. Oestreich, S. Förster and M. Antonietti, *J. Am Chem. Soc*, 1997, **119**, 10116–10120.
83 J. E. Anthony, J. S. Brooks, D. L. Eaton and S. R. Parkin, *J. Am. Chem. Soc*, 2001, **123**, 9482–9483.
84 M. Klues and G. Witte, *CrystEngComm*, 2018, **20**, 63–74.
85 Y. Li, Y. Wu, P. Liu, Z. Prostran, S. Gardner and B. S. Ong, *Chem. Mater*, 2007, **19**, 418–423.
86 D. Loveland, B. Kailkhura, P. Karande, A. M. Hiszpanski and T. Y. Han, *J. Chem. Inf. Model*, 2020, **60**, 6147–6154.
87 S. M. Ryno, C. Risko and J. L. Bredas, *J. Am. Chem. Soc*, 2014, **136**, 6421–6427.
88 K. J. Thorley, T. W. Finn, K. Jarolimek, J. E. Anthony and C. Risko, *Chem. Mater*, 2016, **29**, 2502–2512.
89 M. Zheng, Q. Yang, C. Lu, X. Wu, W. Yan and D. Liu, *Drug Discovery Today*, 2023, **28**, 103598.
90 Y. Tanaka, H. Yoshikawa, T. Asahi and H. Masuhara, *Appl. Phys. Lett*, 2007, **91**, 041102.
91 M. C. Hanna and A. J. Nozik, *J. Appl. Phys*, 2006, **100**, 074510.
92 P. J. Jadhav, P. R. Brown, N. Thompson, B. Wunsch, A. Mohanty, S. R. Yost, E. Hontz, T. V. Voorhis, M. G. Bawendi, V. Bulović and M. A. Baldo, *Adv. Mater*, 2012, **24**, 6169–6174.
93 J. M. M. B. Smith, *Chem. Rev*, 2010, **110**, 6891–6936.
94 W. Shockley and H. J. Queisser, *J. Appl. Phys*, 1961, **32**, 510–519.
95 C. Ramanan, A. L. Smeigh, J. E. Anthony, T. J. Marks and M. R. Wasielewski, *J. Am. Chem. Soc*, 2012, **134**, 386–397.
96 J. B. H. B. D. Folie, S. R. Abramson, J. B. Neaton and N. S. Ginsberg, *J. Am. Chem. Soc*, 2018, **140**, 2326–2335.
97 C. Grieco, E. R. Kennehan, H. Kim, R. D. Pensack, A. N. Brigeman, A. Rimshaw, M. M. Payne, J. E. Anthony, N. C. Giebink, G. D. Scholes and J. B. Asbury, *J. Phys. Chem. C*, 2018, **122**, 2012–2022.
98 K. T. Munson, J. Gan, C. Grieco, G. S. Doucette, J. E. Anthony and J. B. Asbury, *J. Phys. Chem. C*, 2020, **124**, 23567–23578.
99 G. H. Scholes, *J. Phys. Chem. A*, 2015, **119**, 2699–12705.
100 J. Herz, T. Buckup, F. Paulus, J. Engelhart, U. H. F. Bunz and M. Motzkus, *J. Phys. Chem. Lett*, 2014, **5**, 2425–2430.
101 E. Busby, T. C. Berkelbach, B. Kumar, A. Chernikov, Y. Zhong, H. Hlaing, X. Y. Zhu, T. F. Heinz, M. S. Hybertsen, M. Y. Sfeir, D. R. Reichman, C. Nuckolls and O. Yaffe, *J. Am. Chem. Soc*, 2014, **136**, 10654–10660.
102 R. D. Pensack, A. J. Tilley, S. R. Parkin, T. S. Lee, M. M. Payne, D. Gao, A. A. Jahnke, D. G. Oblinsky, P. F. Li, J. E. Anthony, D. S. Seferos and G. D. Scholes, *J. Am. Chem. Soc*, 2015, **137**, 6790–6803.
103 R. D. Pensack, E. E. Ostroumov, A. J. Tilley, S. Mazza, C. Grieco, K. J. Thorley, J. B. Asbury, D. S. Seferos, J. E. Anthony and G. D. Scholes, *J. Phys. Chem. Lett*, 2016, **7**, 2370–2375.
104 N. C. Baird, *J. Am. Chem. Soc*, 1972, **94**, 4941–4948.
105 H. Kim, W. Park, Y. Kim, M. Filatov, C. H. Choi and D. Lee, *Nat. Commun*, 2021, **12**, 5409.
106 H. Ottosson, *Nat. Chem*, 2012, **4**, 969–971.
107 R. Papadakis and H. Ottosson, *Chem. Soc. Rev*, 2015, **44**, 6472–6493.
108 M. Rosenberg, C. Dahlstrand, K. Kilsa and H. Ottosson, *Chem. Rev*, 2014, **114**, 5379–5425.
109 A. R. S. Kandada, A. Petrozza and G. Lanzani, *Phys. Rev. B*, 2014, **90**, 075310.
110 M. Pope and C. E. Swenberg, *Electronic Processes in Organic Crystals and Polymers*, Oxford University Press, New York, 2nd ed., 1999.
111 M. W. B. Wilson, A. Rao, J. Clark, R. S. S. Kumar, D. Brida, G. Cerullo and R. H. Friend, *J. Am. Chem. Soc*, 2011, **133**, 11830–11833.
112 S. R. Yost, J. Lee, M. W. B. Wilson, T. Wu, D. P. McMahon, R. R. Parkhurst, N. J. Thompson, D. N. Congreve, A. Rao, K. Johnson, M. Y. Sfeir, M. G. Bawendi, T. M. Swager, R. H. Friend, M. A. Baldo and T. V. Voorhis, *Nat. Chem*, 2014, **6**, 492–497.
113 B. J. Walker, A. J. Musser, D. Beljonne and R. H. Friend, *Nat. Chem*, 2013, **5**, 1019–1024.
114 Y.-D. Zhang, Y. Wu, Y. Xu, Q. Wang, K. Liu, J.-W. Chen, J.-J. Cao, C. Zhang, H. Fu and H. L. Zhang, *J. Am. Chem. Soc*, 2016, **138**, 6739–6745.
115 J. Zirzlmeier, D. Lehnherr, P. B. Coto, E. T. Chernick, R. Casillas, B. S. Basel, M. Thoss, R. R. Tykwinski and D. M. Guldi, *PNASA*, 2015, **112**, 5325–5330.
116 L. Ma, K. Zhang, C. Kloc, H. Sun, M. E. Michel-Beyerlea and G. G. Gurzadyan, *Phys. Chem. Chem. Phys.*, 2012, **14**, 8307-8312.
117 H. Nagashima, S. Kawaoka, S. Akimoto, T. Tachikawa, Y. Matsui, H. Ikeda and Y. Kobori, *J. Phys. Chem. Lett.*, 2018, **9**, 5855-5861.
118 R. Hayasaka, H. Sakai, M. Fuki, T. Okamoto, R. Khan, M. Higashi, N. V. Tkachenko, Y. Kobori and T. Hasobe, *Angew. Chem. Int. Ed.*, 2024, **63**, e202315747.
119 S. Nakamura, H. Sakai, H. Nagashima, M. Fuki, K. Onishi, R. Khan, Y. Kobori, N. V. Tkachenko and T. Hasobe, *J. Phys. Chem. C*, 2021, **125**, 18287-18296

Open Access Article. Published on 02 June 2026. Downloaded on 6/4/2026 9:29:30 PM.
This article is licensed under a Creative Commons Attribution 3.0 Unported Licence.

Chemical Science Accepted Manuscript

This journal is © The Royal Society of Chemistry 20xx

View Article Online
DOI: 10.1039/D5SC08246C

Supporting data for this article, including experimental methods and characterization data, can be found in the supplementary information (SI).

Open Access Article. Published on 02 June 2026. Downloaded on 6/4/2026 9:29:30 PM.
This article is licensed under a Creative Commons Attribution 3.0 Unported Licence.

Chemical Science Accepted Manuscript